

# Interplay of superconductivity with structural phases in a generalized $t$ - $J$ model

Roland Zeyher<sup>a</sup> and Emmanuele Cappelluti<sup>b</sup>

<sup>a</sup>Max-Planck-Institut für Festkörperforschung, 70569 Stuttgart, Fed. Rep. of Germany

<sup>b</sup>Dipartimento di Fisica, Università di Roma I “La Sapienza”, Piazzale A. Moro, 2, 00185 Roma, Italy

The phase diagram of the  $t - J - V$  model is discussed using a  $1/N$  expansion in terms of  $X$  operators. It is shown that a flux phase of d-wave symmetry is stabilized by the Coulomb interaction at intermediate dopings and competes with d-wave superconductivity. Since the flux wave instability is stronger than the superconducting one optimal doping is essentially determined by the onset of the flux phase at zero temperature at the doping  $\delta_c \sim 0.14$  for  $J/t = 0.3$ . For  $\delta < \delta_c$  the flux phase coexists with superconductivity at low and exists as a single phase at higher temperatures. Due to the different origins of the two instabilities the flux phase boundary and especially  $\delta_c$  is much less sensitive to impurity scattering than the boundary for superconductivity in agreement with experiments in Zn doped  $La - 214$  and  $(Y, Ca) - 123$ .

## 1. INTRODUCTION

The superconducting transition temperature  $T_c$  of many high- $T_c$  superconductors can strongly be suppressed by Zn impurities. Considered as a function of the doping  $\delta$   $T_c$  vanishes finally at a doping  $\delta_{QCP}$  which is the  $T = 0$  endpoint of a line separating a metallic phase at higher doping from a pseudogap phase at lower doping in the  $T - \delta$  plane [1]. The microscopic nature of the pseudogap phase is presently not clear. Since its gap has d-wave symmetry like the superconducting gap it has been suggested that Cooper pairs without long-range phase order are responsible for this phase. On the other hand there is evidence for the occurrence of strong fluctuations in the underdoped regime due to the proximity of phases different from the superconducting phase. At zero temperatures these phases may exhibit a change from long- to short-range order at  $\delta_{QCP}$  so that  $\delta_{QCP}$  is the location of a quantum critical point. One aim of the present investigation is to study the  $t - J - V$  model at large  $N$  to see whether such a quantum critical point scenario applies in this case and what the relevant additional phase is besides of the superconducting one. Another aim is to study the relation between these two phases.

## 2. COMPETITION BETWEEN SUPERCONDUCTIVITY AND FLUX PHASE

We consider a  $t$ - $J$ - $V$  model with  $N$  degrees of freedom per lattice site on a square lattice. Its Hamiltonian can be written in terms of  $X$ -operators as

$$H = - \sum_{\substack{ij \\ p=1\dots N}} \frac{t_{ij}}{N} X_i^{p0} X_j^{0p} + \sum_{\substack{ij \\ p,q=1\dots N}} \frac{J_{ij}}{4N} X_i^{pq} X_j^{qp} \\ + \sum_{\substack{ij \\ p,q=1\dots N}} \left( -\frac{J_{ij}}{4N} + \frac{V_{ij}}{2N} \right) X_i^{pp} X_j^{qq}. \quad (1)$$

The internal labels  $p, q, \dots$  consist of a spin label distinguishing spin up and spin down states and a flavor label counting  $N/2$  identical copies of the original orbital. The coupling constants  $t_{ij}$  and  $J_{ij}$  are confined to nearest neighbors  $i, j$  and simply denoted by  $t$  and  $J$ , respectively. The  $X$  operators satisfy the commutation and anticommutation rules of Hubbard's  $X$  operators for all  $N$ . Moreover, the sum of the diagonal operators is equal to  $N/2$  at each site meaning that only  $N/2$  out of the  $N$  states per site can be occupied simultaneously. The first three terms represent the  $t$ - $J$  Hamiltonian, the last term a screened Coulomb interaction appropriate for two dimensions and

taken from Ref. [2]. In the following we express all energies in units of  $t$  and all lengths in units of the lattice constant of the square lattice. The strength of the Coulomb interaction will be characterized by its value between nearest neighbor sites  $V_{nn}$ .

The self-energy  $\Sigma$  of the one-particle Green's function is independent of frequency at large  $N$  and has the general form [3]

$$\Sigma(\mathbf{k}, \mathbf{q}) = \Sigma(\mathbf{k})N_c\delta(\mathbf{q}) + \phi(\mathbf{k}, \mathbf{q}). \quad (2)$$

$\Sigma(\mathbf{k})$  denotes the self-energy in the normal state.  $\phi$  is an additional contribution describing a new ground state characterized by the modulation wave vector  $\mathbf{q}$ . For the determination of phase boundaries  $\phi$  can be considered as infinitesimally small. Calculating explicitly the self-energy from Eq.(1) one finds

$$\phi(\mathbf{k}, \mathbf{q}) = \sum_{\alpha} f_{\alpha}(\mathbf{q})F_{\alpha}(\mathbf{k}, \mathbf{q}), \quad (3)$$

with  $\vec{F}(\mathbf{k}, \mathbf{q}) = (t(\mathbf{k} - \mathbf{q}), 1, J \cos(k_x), J \sin(k_x), J \cos(k_y), J \sin(k_y))$ , and  $f_{\alpha}$  satisfying the homogeneous system of equations

$$\sum_{\beta} [\delta_{\alpha\beta} - a_{\alpha\beta}(\mathbf{q})] f_{\beta}(\mathbf{q}) = 0. \quad (4)$$

The matrix elements  $a_{\alpha\beta}(\mathbf{q})$  in Eq. (4) are defined by

$$a_{\alpha\beta}(\mathbf{q}) = \frac{1}{N_c} \sum_{\mathbf{p}} T \sum_n G_{\alpha}(\mathbf{p}, \mathbf{q}) F_{\beta}(\mathbf{p}, \mathbf{q}) \cdot g_0(\mathbf{p}, i\omega_n) g_0(\mathbf{p} - \mathbf{q}, i\omega_n), \quad (5)$$

with  $\vec{G}(\mathbf{k}, \mathbf{q}) = (1, t(\mathbf{k}) + V(\mathbf{q}) - \frac{J(\mathbf{q})}{2}, -\cos(k_x), -\sin(k_x), -\cos(k_y), -\sin(k_y))$ , and  $g_0(\mathbf{p}, i\omega_n) = 1/(i\omega_n - \Sigma(\mathbf{p}))$ . The boundary between the normal state and a possible new phase corresponds to a nontrivial solution for  $f_{\beta}$  of Eq.(4). In this way both the modulation vector  $\mathbf{q}$  and the components of the order parameter in the six-dimensional order parameter space is determined.

Putting first  $V = 0$  and decreasing doping or temperature from large values we find for  $J < 1$  a first instability of the normal state with respect to the flux phase order parameter

$$\phi_{FL}(\mathbf{k}, P\mathbf{Q}) \sim i(\cos(k_x) - \cos(k_y)). \quad (6)$$

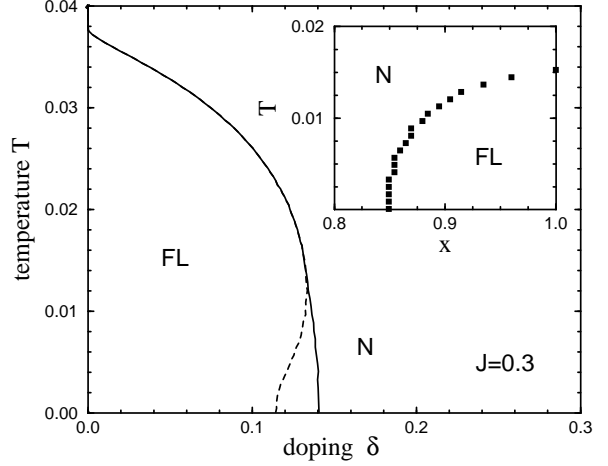


Figure 1. Incommensurate (solid line) and commensurate (dashed line) phase boundaries in the  $T - \delta$  plane. Insert: Instability vector  $\mathbf{Q} = (1, x)\pi$  as a function of  $T$ .

The solid line in Fig. 1 shows the corresponding instability line for  $J = 0.3$  in the  $T - \delta$  plane. Writing the modulation vector as  $\mathbf{Q} = \pi(1, x)$  the inset of Fig. 1 shows  $x$  as a function of temperature along the instability line. For  $T > 0.015$  the flux phase is commensurate with the wave vector  $\mathbf{Q}_c = \pi(1, 1)$ , for  $T < 0.015$  one wave vector component is incommensurate. Fixing  $\mathbf{Q}$  to the commensurate value  $\mathbf{Q}_c$  for all temperatures the instability line is given for  $T < 0.015$  by the dashed line in Fig. 1 describing a reentrant behavior of the normal state between  $\delta = 0.12$  and  $0.14$ . This feature is an artefact caused by the assumption of a commensurate phase at all temperatures. At zero temperature the critical doping  $\delta_c$  is a monotonic function of  $J$ , with  $\delta_c = 0$  for  $J = 0$ ,  $\delta_c \sim 0.14$  for  $J = 0.3$  and  $\delta_c \sim 0.20$  for  $J = 0.6$ . Thus  $\delta_c$  is near the experimental value for optimal doping and denotes a quantum critical point because the incommensurate flux phase has short-range order for any finite temperature if fluctuations are taken into account.

The flux phase is unstable at very low dopings with respect to dimers [4]. Another instability line, indicated by the dot-dashed curve in the upper panel of Fig. 2, describes a diverging compressibility of the normal state, i.e., the region to

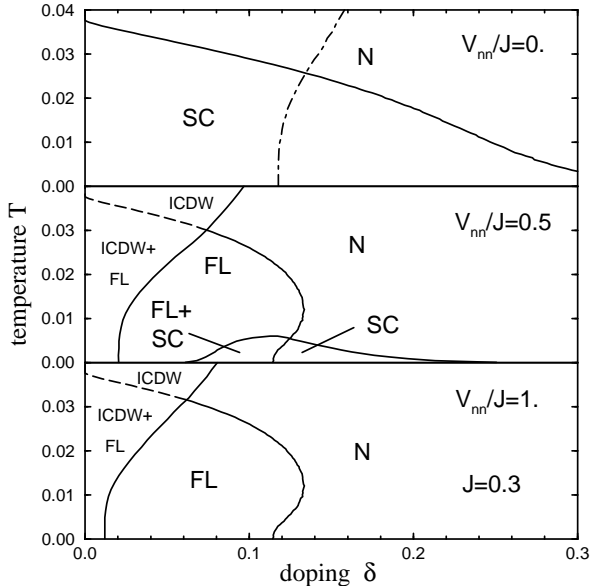


Figure 2. Phase diagram for  $J = 0.3$  and different Coulomb interaction strengths  $V_{nn}$ .  $N, FL, SC, ICDW$  denote the normal, flux, superconducting, and CDW phase, respectively, the dot-dashed line in the upper panel a diverging compressibility in the normal state.

the left of this line would show phase separation in the normal state. Since the flux phase falls inside the phase separation regime, the solid line in Fig. 1 has no physical meaning in the case  $V = 0$ .

The instability line of the normal state towards superconductivity has been discussed in Ref [5]. In the BCS-approximation  $T_c$  is  $\sim \exp(1/\lambda_i)$ , where  $\lambda_i$  is the lowest eigenvalue of the static kernel of the linearized gap equation and  $i$  denotes one of the 5 representations of the point group  $C_{4v}$  of the square lattice. Only  $\lambda_3$  corresponding to d-wave symmetry exhibits strong negative values. It even diverges at  $\delta_c$  due to critical fluctuations caused by the incipient flux phase. The numerical solution for  $T_c$ , which also takes into account retardation, however, shows that critical fluctuations have only little influence on  $T_c$  and that  $T_c$  is mainly determined by the instantaneous term. Keeping only this term the solid line in the upper panel of Fig. 2 shows  $T_c$  as a function of  $\delta$ . Interesting is that the superconducting unlike the normal state is stable against phase separation.

Taking also the Coulomb interaction  $V$  into ac-

count phase separation is no longer possible but charge density waves (CDW) may be stabilized. The two lower panels of Fig. 2 show, however, that CDW's may be only stable at rather low dopings far away from optimal doping and are thus of less interest for the following. In order to be able to discuss fully the interplay between superconductivity and the flux phase we treat the corresponding order parameters in a nonlinear way, assuming only that the flux phase is commensurate. The self-consistent equations are then  $4 \times 4$  matrix equations which are most conveniently formulated using a Nambu representation with 4 states.

The middle panel of Fig. 2 shows the phase diagram for  $V_{nn}/J = 0.5$ . For  $\delta > \delta_c$   $T_c$  is monotonically increasing with decreasing  $\delta$  similar as in the upper panel, only its absolute value is reduced because of the repulsion  $V_{nn}$ . Below the onset of the flux phase at  $\delta_c$  superconductivity and the flux phase compete with each other because both have d-wave symmetry. Since the nesting instability leading to the flux phase is stronger than the superconducting instability the flux phase suppresses strongly  $T_c$  with decreasing  $\delta$  below  $\delta_c$ . As a result  $T_c$  assumes a maximum just below  $\delta_c$  and decreases both towards lower and higher dopings. Optimal doping is thus determined at large  $N$  by the onset of the flux phase at  $\delta_c$ . For  $\delta < \delta_c$  the flux and the superconducting phase coexist for  $T < T_c$  whereas the flux phase alone is stable for  $T_c < T < T^*$ , forming there a pseudogap phase with a d-wave gap in the single particle spectrum. The lower panel in Fig. 2 shows the phase diagram for  $V_{nn}/J = 1$ . The Coulomb repulsion is now strong enough to suppress completely  $T_c$ . The region of CDW states has been shifted further towards smaller doping and the flux phase covers a large region to the left of the normal state.

### 3. PHASE DIAGRAM IN THE PRESENCE OF IMPURITY SCATTERING

Both the flux and the superconducting phase have d-wave symmetry. Their phase boundaries  $T^*$  and  $T_c$ , respectively, thus should be sensitive to impurity scattering. Experimentally this holds

in the case of Zn impurities for  $T_c$  but practically not for  $T^*$  [1]. From a theoretical point of view  $T_c$  and  $T^*$  may depend differently on impurity scattering because the underlying instabilities are quite different. For instance, nesting effects play an important role in the case of  $T^*$  but not in the case of  $T_c$ .

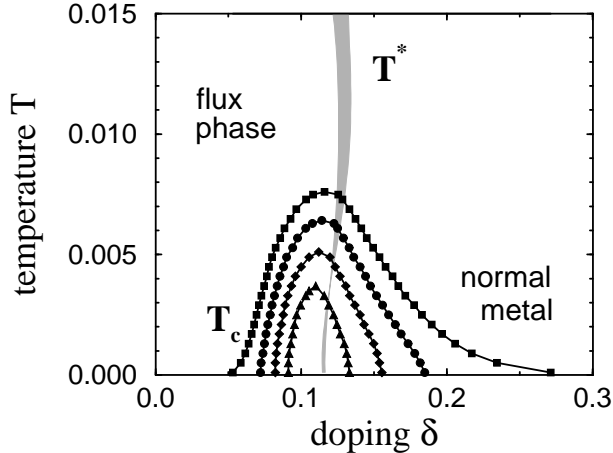


Figure 3. Solid lines: Suppression of  $T_c$  by impurity scattering, calculated with the scattering rates  $\Gamma = 0$  (squares),  $2 \cdot 10^{-3}$  (circles),  $4 \cdot 10^{-3}$  (diamonds), and  $6 \cdot 10^{-3}$  (triangles). Grey region: Corresponding variation of the transition temperature  $T^*$  to the flux state.

In a simple approximation, the effects of impurities in the normal state can be taken into account by introducing a renormalized frequency

$$i\tilde{\omega}_n = i\omega_n + i\Gamma \frac{\omega_n}{|\omega_n|}, \quad (7)$$

where  $\Gamma$  is a scattering rate, here used as a free parameter proportional to the impurity concentration. Throughout the flux phase the self-energy due to impurity scattering is still diagonal in the  $4 \times 4$  Nambu representation because the flux order parameter does not couple to the impurities. The constant  $\Gamma$  in Eq. (7) accounts in a phenomenological way both for weak and strong potential scattering by impurities. The interesting doping region for superconductivity is in our model rather far away from the Van Hove singularity, so that the band can be assumed to be structureless and  $\Gamma$  to be independent of frequency.

The solid lines in Fig. 3 show numerical results for  $T_c$  as a function of doping  $\delta$  for different scattering rates  $\Gamma$ , using  $J = 0.3$  and  $V_{nn} = 0.5J$ . These curves illustrate the suppression of  $T_c$  with increasing scattering rates  $\Gamma = 0, 2 \cdot 10^{-3}, 4 \cdot 10^{-3}$ , and  $6 \cdot 10^{-3}$ . The corresponding changes in  $T^*$ , determining the phase boundary between the normal state and the flux state, are depicted in Fig. 3 by the grey region. The chosen values for  $\Gamma$  correspond roughly to  $\Gamma \simeq 1.0T_c$  at optimal doping, and to  $\Gamma \simeq 1.5T_c$  in the strongly underdoped region, interpolating between the weak- and the strong-coupling regimes. One important result of Fig. 3 is that the flux phase boundary  $T^*$  is only slightly shifted by impurities, in spite of the strong suppression of the superconducting critical temperature. In particular, the critical doping  $\delta_c$  at zero temperature is almost completely independent of the impurity scattering rate. Since in our approach the maximum of  $T_c$  as a function of doping is essentially determined by  $\delta_c$  this means that the  $T_c(\delta)$  curves shrink to  $\delta_c$  with increasing scattering rate which is a characteristic feature of Fig. 3. Interpreting Fig. 3 in terms of a quantum critical point scenario means that the corresponding critical doping  $\delta_{QCP}$  is given by  $\delta_c$  and that  $\delta_{QCP}$  is nearly completely independent of the impurity scattering rate. The curves in Fig. 3 are in excellent agreement with the corresponding experimental curves in Zn doped (Y,Ca)-123 and La-214, as given in Fig. 2 of Ref.[1].

## REFERENCES

1. J.L. Tallon, C. Bernhard, G.V.M. Williams, and J.W. Loram, Phys. Rev. Lett. 79 (1997) 5294.
2. F. Becca, M. Tarquini, M. Grilli, and C. Di Castro, Phys. Rev. B 54 (1996) 12 443.
3. E. Cappelluti and R. Zeyher, Phys. Rev. B 59 (1999) 6475.
4. E. Ercolessi, P. Pieri, and M. Roncaglia, Phys. Lett. A 225 (1997) 331.
5. R. Zeyher and A. Greco, Eur. Phys. J. B 6 (1998) 473.